INTERNATIONAL JOURNAL FOR NUMERICAL METHODS IN FLUIDS, VOL. 17, 731–754 (1993)

ON THE INSTABILITY OF A FULL NON-PARALLEL FLOW—KOVASZNAY FLOW

H. B. CHEN*

Department of Applied Science, Red Deer College, Red Deer, Alberta T4J 5H5, Canada

SUMMARY

The local instability of a full non-parallel flow is investigated. The basic flow is a horizontal uniform flow about a vertical array of periodic bound eddies. This flow was found by Kovasznay as an exact solution to the Navier–Stokes equations. The problem is formulated as an initial value problem with two sets of complete orthogonal functions. A new approach to the problem with semi-infinite domain is given computationally with a new modified rational Chebyshev function. The linear stability analysis of the Kovasznay flow is performed with respect to the odd–rational Chebyshev mode and the even–rational Chebyshev mode for the evolution of disturbances. While symmetrical vortex sheets appeared through the process of big eddies breaking into small eddies in the odd–rational Chebyshev mode, the von Kármán vortex street phenomena is found in the even–rational Chebyshev mode. The mode corresponding to antisymmetric velocity perturbation is found to be far more unstable than symmetric disturbance. An organized structure is developed after the onset of instability. Several general characteristics of non-parallel flow stability are discussed.

KEY WORDS Instability Non-parallel flow Fourier–rational Chebyshev mode Vortex street

1. INTRODUCTION

A given flow, the stability of which is to be investigated, is called the basic flow or basic state. The basic flow can be classified into the following categories: (a) parallel flow $\mathbf{v}=(U(y), 0, 0)$; (b) nearly parallel flow $\mathbf{v}=(U(x, y), V(x, y), 0)$, $V(x, y) \ll U(x, y)$ and $\partial U/\partial x \ll 1$; (c) full non-parallel flow $\mathbf{v}=(U(x, y), V(x, y), 0)$ or $\mathbf{v}=(U(x, y, z), V(x, y, z), W(x, y, z))$ in three dimensions.

Methods of analysing the stability of parallel flows were formulated in the beginning of this century. Orr and Sommerfeld derived the celebrated equation that provides the basis of the linear stability theory of parallel flow motions. The assumption of parallel flows dramaticaly simplifies the problem mathematically. The theory of stability of parallel flows indeed has played a significant role in the process of understanding hydrodynamic stability phenomena and enriched the hydrodynamic stability theory itself. However, most external flows of practical interest are non-parallel, the parallel flow assumption is of questionable validity.[1] In order to understand the transition to turbulence beyond the parallel theory, insight can be reached with either non-parallelism or non-linearity.[2] While richness of non-linearity has been paid a lot of attention, the importance of non-parallelism is just gradually being realized.

A fluid motion having a mean flow which varies both in the direction of the mean flow and in the direction perpendicular to it is defined as non-parallel flow. Its stability problem is called

* Current Address: Advanced Laser and Fusion Technology, Inc., 189 Deveault Street, Unit 7, Hull, Quebec J8Z IT9, Canada.

0271–2091/93/210731–24$17.00

Received March 1992
Revised December 1992

non-parallel flow stability. There is a real need for studying stability of non-parallel flow in order to understand better the flow phenomena of practical interest. In the stability analysis of non-parallel flows, it is usually assumed that the flow is locally parallel in space. However, difficulties associated with this assumption were recognized by Tatsumi and Kakutami[3] and Lanchon and Eckhaus[4] among others. Efforts to rationalize the assumption with the asymptotic method of multiple scale can be found in the works of Bouthier,[5] Ling and Reynolds,[6] Gaster,[7] Saric and Nayfeh,[8] Smith,[9] Hall,[10,11] Asrar and Nayfeh.[12] The effects of non-parallel correction can be found in the works of Wakitani,[13] Gotoh *et al.*,[14] Chomaz *et al.*,[15] Karniadakis and Triantaflyllou[16] and the reference list at the end. Energy stability analysis of non-parallel flow can be found in the works of Lin and Tobak[17,18] and Coscia.[19]

The stability of full non-parallel flows suffers from some serious uncertainties associated with the approximate nature of the basic states of non-parallel flows. As pointed out by Drazin and Reid,[20] in dealing with the stability of non-parallel flows, there are two major problems: the first is concerned with obtaining a suitably accurate description of the basic flow, while the other is concerned with obtaining approximations to the solution of the partial differential equations which govern the disturbance flow. In order to overcome the difficulty and concentrate on stability analysis, it is desirable to have some stability analyses of non-parallel flows which are exact solutions of the Navier–Stokes equations. Taylor[21] intuitively obtained an exact solution to the Navier–Stokes equations which represents a double array of vortices. Kovasznay[22] obtained an exact steady-flow solution in a similar manner by assuming that vorticity is proportional to stream function. The flow is periodic in one direction (which Beaumout[23] and Gotoh *et al.*,[14] called spatially periodic flow in z-direction) and semi-infinite in another direction. Kovasznay suggested that the flow may be used to describe the flow downstream of a two-dimensional grid (we note that Prosperetti[24] obtained a similar solution to describe the laminar flow at large distances from an infinite two-dimensional grid). This steady solution provides us with an opportunity to study the mechanism of the non-parallel flow stability. The results obtained will then be free from concern about the accuracy of the basic state. The basic flow is given in Section 2.1. The disturbance equations are given in Section 2.2. Stability analyses of normal mode approaches for non-parallel flow are discussed in Section 2.3. An initial value problem for the linear instability of the Kovasznay flow is formulated in Sections 3.1. and 3.2. The numerical method for the disturbance equation and self-consistency test are described in Section 3.3. The results and discussion are given in Section 4, and finally a conclusion in Section 5.

2. STABILITY ANALYSIS

2.1. Basic flow

The basic flow to be studied here is the Kovasznay flow, which is an exact solution of the Navier–Stokes equation and represents a full non-parallel flow. A streamline pattern of this flow is depicted in Figure 1, where the length is normalized with the spatial period, d, of the periodic bound eddies. The flow far downstream from these eddies approaches a uniform stream of speed U. The stream function normalized with Ud of the Kovasznay flow $\bar{\psi}$ is given by

$$\bar{\psi} = z - B \sin(2\pi z) \exp(\mathbb{M}x), \tag{1}$$

where (x, z) are the Cartesian co-ordinates, B is a parameter which determines the size of the wake bubble and $\mathbb{M}$ is given by

$$\mathbb{M} = \tfrac{1}{2}(\mathbb{R} - \sqrt{(\mathbb{R}^2 + 16\pi^2)}).$$

where $\mathbb{R} = U_d/\nu$.

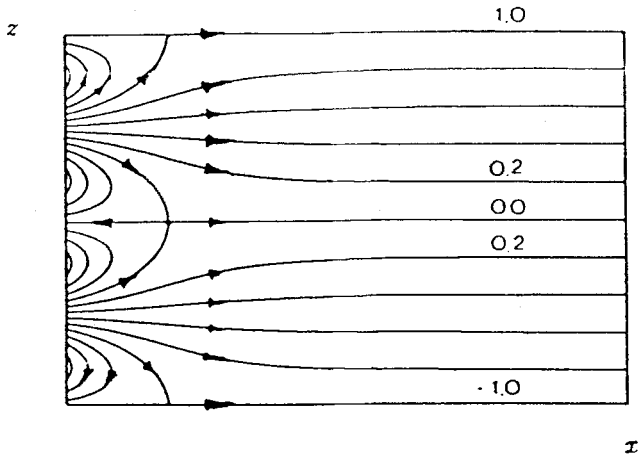

Figure 1. Basic flow: Kovasznay flow ($\mathbb{R}=40$, $B=1$)

Kovasznay suggested that the solution corresponding to the negative root of $\mathbb{M}$ above can be used to describe the wake flow in the region $x>0$ behind a grid of wires with a uniform spacing d at $x=0$. Note that the length of the wake, i.e. the distance between $x=0$ and stagnation point, is given by

$$l=\frac{1}{\mathbb{M}}\ln\left(\frac{1}{2\pi B}\right).$$

Since $\mathbb{M}<0$, we must have $2\pi B>1$ for the existence of the closed wake shown in Figure 1. When $B=0$, the flow is a uniform stream of speed U in the x-direction. Further physical interpretation of the flow can be found in Prosperetti.[24]

2.2. *Disturbance equation*

Let the perturbed stream function ϕ be written as

$$\phi=\bar{\psi}+\psi,$$

where $\bar{\psi}$ is the basic state stream function and ψ is the stream function perturbation. Substituting the above into Navier–Stokes equation and neglecting non-linear terms, we have the disturbance equation which is the governing equation for the linear stability with the basic state given by equation (1) as

$$\left(\partial_t-\frac{1}{\mathbb{R}}\nabla^2\right)\nabla^2\psi=\bar{\psi}_x\nabla^2\psi_z-\bar{\psi}_z\nabla^2\psi_x+\psi_x\nabla^2\bar{\psi}_z-\psi_z\nabla^2\bar{\psi}_x. \tag{2}$$

2.3. *Normal mode approach*

The first and usual approach in stability analysis of parallel flow is to seek a disturbance solution of the form

$$\psi(x, z, t)=\eta(z)e^{i(kx-\sigma t)}$$

and solve the resulting problem for spatial eigenvalue k and temporal eigenvalue σ. In non-parallel case, it is well known that no spatial eigenvalues exist, so we assume the disturbance solution of the form

$$\psi(x, z, t)=\eta(x, z)A(t), \qquad A(t)=e^{\sigma t}. \tag{3}$$

Gotoh *et al.*[14] predicted much more difficulty with the above eigenvalue problem than the parallel case. Lagnado *et al.*[25] circumvent the problem by seeking an alternating representation of the solution. In this section, I like to elaborate in more detail.

Substituting (3) into the governing equation (2), we formulate the eigenvalue problem of Kovasznay flow using the spectral Galerkin method. It is found that when $B=0$, at which flow is of parallel case, all real parts of the eigenvalues are negtive. Physically it is stable, as expected, since the flow is uniform. However, when $B>0$, at which flow is a non-parallel case (where our main interests are), it is found after extensive and careful study that there are no convergent eigenvalues.

Kovasznay flow possesses two characteristics which prevent us from finding unique eigenvalues. Computationally, the flow domain is semi-infinite ($0<x<\infty$). For a semi-infinite domain, referring to Grosch and Salwen's work,[26] Craik[27] mentioned that no eigenvalue exist for a simple one-dimensional wave equation for ($0<x<\infty$). Theoretically, the characteristic of non-parallelism keeps us from finding the convergent eigenvalues. In study of the stability of a large gas bubble rising through liquid, of which basic state is a non-parallel flow, Batchelor[28] showed that neither eigenmodes of disturbance whose amplitude vary exponentially with respect to time exist nor do spatial eigenmodes. Consequently, he turns his attention to analyse the evolution of a disturbance in arbitrary initial form. In studying the Rossby waves in a shear flow with critical level, Tung[29] resolved the dilemma of normal mode approach by solving an initial value problem. A similar approach can be found in the work of Carrier and Chang.[30] Lagnado *et al.*[25] claimed that the initial value problem is more general in the sense that the initial disturbance is left unspecified. Normal mode is a special form of the solution. If one observes the form of the solution more carefully, one finds that it is assumed that not only is the solution separatable, but also in a special form: an exponential growth or decay form. Due to the unbounded domain and non-parallelism of Kovasznay flow and our computation of eigenvalue approach, we conclude that no spatial and temporal eigenvalues exist for the flow. So we seek the solution in an initial value problem approach and study the evolution of the disturbances.

3. FORMULATION OF INITIAL VALUE PROBLEM APPROACH

We are going to solve the disturbance equation (2) by using the spectral Galerkin method as an initial value problem.

3.1. Fourier mode in z

Note that the basic state is spatially periodic in z-direction, we seek the solution of (2) in the form of the Fourier mode in z-direction

$$\psi=\sum_{n=1}^{N+1} F_n(t, x)\sin\frac{2n\pi z}{\lambda}+\sum_{n=1}^{N+1} G_n(t, x)\cos\frac{2(n-1)\pi z}{\lambda}, \tag{4}$$

where $F_n(t, x)$ and $G_n(t, x)$ are unknown functions of t and x and λ is the wavelength in the z-direction. A particular interest is the case $\lambda=1$, when the instability does not discriminate

against any particular bound eddy. It will be assumed that the disturbance does not enter the flow at $x=0$, it vanishes at $x=\infty$ (Reference 31), i.e.

$$(u, w)=0 \quad \text{at } x=0 \text{ and } x=\infty.$$

Thus, the instability is entirely due to the energy transfer from the basic state to the disturbance within the flow domain. (An approach with more challenging inflow/outflow boundary condition is on the way.) The boundary conditions corresponding to $F_n(t, x)$ and $G_n(t, x)$ will shortly be derived when the form of their solutions are chosen.

The function $F_n(t, x)$ and $G_n(t, x)$ will be determined by successive Galerkin projections. First substituting (4) into (2), multiplying the resulting equation with $\sin 2m\pi z/\lambda$, and integrating over one wavelength λ, we have the the odd mode equation

$$\left\{\left[\partial_t-\left(\frac{1}{\mathbb{R}}\right)E_m^2\right]E_m^2+E_m^2 D\right\}F_m=B[-\pi(m+\lambda)\bar{\psi}_{x0}(E_{m+1}^2-\mathbb{N})+\tfrac{1}{2}\bar{\psi}_{z0}(E_{m+1}^2-\mathbb{N})D]F_{m+\lambda}$$
$$+B[\pi(m-\lambda)\bar{\psi}_{x0}(E_{m-1}^2-\mathbb{N})+\tfrac{1}{2}\bar{\psi}_{z0}(E_{m-1}^2-\mathbb{N})D]F_{m-\lambda}, \quad (5)$$

where $E_m^2=\partial_{xx}-(2m\pi/\lambda)^2$, $\mathbb{N}=\mathbb{M}^2-(2\pi)^2$, $D=\partial_x$ and m varies from 1 to $M+1$.

Similarly, the Galerkin projection with the even Fourier component $\cos[2(m-1)\pi z]/\lambda$ yields

$$\left\{\left[\partial_t-\left(\frac{1}{\mathbb{R}}\right)E_{m-1}^2\right]E_{m-1}^2+E_{m-1}^2 D\right\}G_m=B[\tfrac{1}{2}\bar{\psi}_{z0}D-(m+\lambda-1)\pi\bar{\psi}_{x0}](E_{m+\lambda-1}^2-\mathbb{N})G_{m+\lambda}$$
$$+B[\tfrac{1}{2}\bar{\psi}_{z0}D+(m-\lambda-1)\pi\bar{\psi}_{x0}](E_{m-\lambda-1}^2-\mathbb{N})G_{m-\lambda}. \quad (6)$$

Hence, the amplitudes of odd and even Fourier modes (F_n and G_n) are decoupled, as they are governed independently by (5) and (6), respectively.

3.2. A new approach in the x-direction: rational Chebyshev mode

The problem with an unbounded domain is a difficult one computationally. One of many difficulties is the lack of a well-behaved base function. Continuing with the earlier work by Orszag and Boyd, Boyd[32] recently defined a new spectral basis, the 'rational Chebyshev functions on the semi-infinite interval', which is related to the Chebyshev polynomial by a mapping. It is shown that these rational functions inherit most of the good numerical characteristics of the Chebyshev polynomials: orthogonality, completeness, exponential of 'infinite order' convergence, matrix sparsity for equations with polynomial coefficients and simplicity, which provides a far better behaved basis function for spectral method in semi-infinite domain than the Laguree function. In the present work, since we have a semi-infinite domain in x-direction, we are using the new functions as basis functions in x-direction.

The amplitude of each Fourier component will be expanded in series of the rational Chebyshev function TL_k:

$$F_m=A_m^k(t)TL_k(x). \quad (7)$$

The new basis function, $TL_k(x)$, $x\in(0, \infty)$ is defined by

$$TL_k(x)\equiv T_k(\xi)\equiv\cos(k\theta),$$

where $T_k(\xi)$ is the ordinary Chebyshev function, and the three co-ordinates are related by

$$x\equiv(1+\xi)/(1-\xi), \qquad \xi\equiv(x-1)/(x+1),$$
$$x\equiv\cot^2(\theta/2), \qquad \theta=2\operatorname{arccot}(\sqrt{x}).$$

It is easily verified that the rational Chebyshev function has the following orthogonality property with weighting function $1/[(x+1)x^{1/2}]$

$$\int_0^\infty TL_m(x)TL_n(x)\frac{1}{[(x+1)x^{1/2}]}\,dx=\int_0^\pi \cos(m\theta)\cos(n\theta)\,d\theta$$

$$=\begin{cases}\pi, & m=n=0,\\ 0, & m\neq n\\ \pi/2, & m=n>0.\end{cases}$$

To obtain a system of ordinary differential equations for $A_m^k(t)$, we first substitute (7) into (5), and obtain

$$\dot{L}_{m1}(A_m^k(t)TL_k(x))=B\mathbb{R}[L_{m2}(A_{m-1}^k(t)TL_k(x))+L_{m3}(A_{m+1}^k TL_k(x))], \tag{8}$$

where

$$\dot{L}_{m1}=(\mathbb{R}\partial_t-E_m^2)E_m^2+\mathbb{R}E_m^2D,$$

$$L_{m2}=\pi(m-\lambda)\bar{\psi}_{x0}(E_{m-1}^2-\mathbb{M})+\tfrac{1}{2}\bar{\psi}_{z0}(E_{m-1}^2-\mathbb{M})D,$$

$$L_{m3}=-\pi(m+\lambda)\bar{\psi}_{x0}(E_{m+1}^2-\mathbb{M})+\tfrac{1}{2}\bar{\psi}_{z0}(E_{m+1}^2-\mathbb{M})D.$$

The x-dependence in (8) can be eliminated by the Galerkin projection of (8) onto TL_l with the above-mentioned weight function

$$\int_0^\infty \text{eq.(8)}\cdot(TL_l)(x)\bar{W}(x)\,dx=0,$$

where l is from 0 to K. The projection yields the system for the odd mode,

$$\mathbb{R}\bar{R}_{mkl}\dot{A}_m^k(t)=Q_{mkl}A_{m-1}^k(t)+R_{mkl}A_m^k(t)+S_{mkl}A_{m+1}^k(t), \tag{9}$$

where the upper dot denotes time differentiation, and

$$Q_{mkl}=B\mathbb{R}\int_0^\infty (TL_l)\bar{W}L_{m2}(TL_k)\,dx,$$

$$R_{mkl}=-\int_0^\infty (TL_l)\bar{W}L_{m1}(TL_k)\,dx,$$

$$S_{mkl}=B\mathbb{R}\int_0^\infty (TL_l)\bar{W}L_{m3}(TL_k)\,dx.$$

The above integrals can be reduced to definite integrals between $\theta=0$ and $\theta=\pi$, by use of the transformation mentioned above.

For any given m, the coefficients of A_m^k in (9) are $(M+1)$ by $(K+1)$ matrices. Hence, operating both sides of (9) with the inverse of $\bar{R}_{mkl}$ for each integer m in $1\leqslant m\leqslant M$, we have

$$\dot{A}_m^k(t)=q_{mkl}A_{m-1}^k(t)+r_{mkl}A_m^k(t)+s_{mkl}A_{m+1}^k(t) \tag{10}$$

where

$$(q_{mkl}, r_{mkl}, s_{mkl})=(\mathbb{R}\bar{R}_{mkl})^{-1}(Q_{mkl}, R_{mkl}, S_{mkl}).$$

Thus, (10) is a system of $(M+1)$ $(K+1)$ equations in which $(M+1)(K+1)$ are unknowns. However, there are additional $3(M+1)$ equations which arise from the boundary conditions needed to be satisfied:

$$u|_{x=0}=\left.\frac{\partial\psi}{\partial z}\right|_{x=0}=0, \qquad u|_{x=\infty}=\left.\frac{\partial\psi}{\partial z}\right|_{x=\infty}=0,$$

$$w|_{x=0}=-\left.\frac{\partial\psi}{\partial z}\right|_{x=0}=0, \qquad w|_{x=\infty}=\left.\frac{\partial\psi}{\partial x}\right|_{x=\infty}=0.$$

By use of the following relations:

$$u=\frac{\partial\psi}{\partial z}=\sum_{m=1}^{M+1}\frac{2m\pi}{\lambda}\cos\frac{2m\pi z}{\lambda}\sum_{k=0}^{K}TL_k(x)A_m^k(t),$$

$$w=-\frac{\partial\psi}{\partial x}=-\sum_{m=1}^{M+1}\sin\frac{2m\pi z}{\lambda}\sum_{k=0}^{K}\left(\frac{\mathrm{d}}{\mathrm{d}x}TL_k(x)\right)A_m^k,$$

$$TL_k|_{x=0}=(-1)^k, \qquad TL_k|_{\infty}=1, \qquad \frac{\mathrm{d}TL_k}{\mathrm{d}x}|_{x=0}=k^2(-1)^k, \qquad \frac{\mathrm{d}TL_k}{\mathrm{d}x}|_{x=\infty}=0,$$

we have the following equations for boundary conditions for u at $x=0$,

$$\sum_{k=0}^{K}(-1)^kA_m^k=0, \tag{11}$$

and for $ux=\infty$

$$\sum_{k=0}^{K}A_m^k=0, \tag{12}$$

and for w at $x=0$

$$\sum_{k=0}^{K}k^2(-1)^kA_m^k=0, \tag{13}$$

for each $1\leqslant m\leqslant M+1$. The condition $w=0$ at $x=\infty$ is automatically satisfied because of $\mathrm{d}TL_k/\mathrm{d}x|_{x=\infty}=0$. Hence, we have $(M+1)(K+1)+3(M+1)$ equations from (10)–(13) with only $(M+1)(K+1)$ unknowns. To render the above system determinate, we adopt a Tau method[3] by replacing the last three equations in (10) with (11)–(13) for each m. That is to say, we form the Galerkin projection in the flow direction only up to $[(K+1)-3)]$. So, we have $(M+1)[(K+1)-3)]+3(M+1)=(M+1)(K+1)$ equations in $(M+1)(K+1)$. Readers are referred to Chen[34] for more detail and general systematical use of Tau method to deal with boundary conditions in spectral Galerkin method.

The final system of ODE can be written as

$$[\dot{V}]=[E][V], \tag{14}$$

where the upper dot denotes differentiation with respect to time and

$$[V]^{\mathrm{T}}=(A_1^k, A_2^k, \ldots, A_{m-1}^k, A_m^k, \ldots, A_M^k, A_{M+1}^k),$$

and

$$[E]=\begin{bmatrix} r_{1kl} & s_{1kl} & & & & & \\ q_{2kl} & r_{2kl} & s_{2kl} & & & & \\ & q_{3kl} & r_{3kl} & s_{3kl} & & & \\ & & \ddots & \ddots & \ddots & & \\ & & & & & q_{(M+1)kl} & r_{(M+1)kl} \end{bmatrix},$$

where

$$r_{mkl}=\begin{bmatrix} r_{m00} & r_{m10} & \cdots & r_{mK0} \\ r_{m01} & r_{m11} & \cdots & r_{mK1} \\ & & \vdots & \\ r_{m0(K-3)} & r_{ml(K-3)} & \cdots & r_{mK(K-3)} \\ 1 & -1 & \cdots & (-1)^K \\ 1 & 1 & \cdots & 1 \\ 0 & -1 & \cdots & K^2(-1)^K \end{bmatrix}$$

$$q_{mkl}=\begin{bmatrix} q_{m00} & q_{m10} & \cdots & q_{mK0} \\ q_{m01} & q_{m11} & \cdots & q_{mK1} \\ & & \vdots & \\ q_{m0(K-3)} & q_{m1(K-3)} & \cdots & q_{mK(K-3)} \\ 0 & 0 & \cdots & 0 \\ 0 & 0 & \cdots & 0 \\ 0 & 0 & \cdots & 0 \end{bmatrix}$$

$$S_{mkl}=\begin{bmatrix} S_{m00} & S_{m10} & \cdots & S_{mK0} \\ S_{m01} & S_{m11} & \cdots & S_{mK1} \\ & & \vdots & \\ S_{m0(K-3)} & S_{m1(K-3)} & \cdots & S_{mK(K-3)} \\ 0 & 0 & \cdots & 0 \\ 0 & 0 & \cdots & 0 \\ 0 & 0 & \cdots & 0 \end{bmatrix},$$

equation (14) with a set of initial conditions constitutes an initial value problem for the evolution of the disturbances.

Similarly, the governing equation of the initial value problem for the even mode disturbances is found to be

$$[\dot{U}]=[\bar{E}]\ [U], \tag{15}$$

where

$$[U]^{\mathrm{T}}=(B_1^k, B_2^k, \ldots, B_{m-1}^k, B_m^k, \ldots, B_M^k, B_{M+1}^k)$$

and the submatrices in $[\bar{E}]$ has similar structure as in $[E]$.

The overstructure of projection by using the spectral method is shown in Table I.

Table I. Overstructure of Galerkin projection

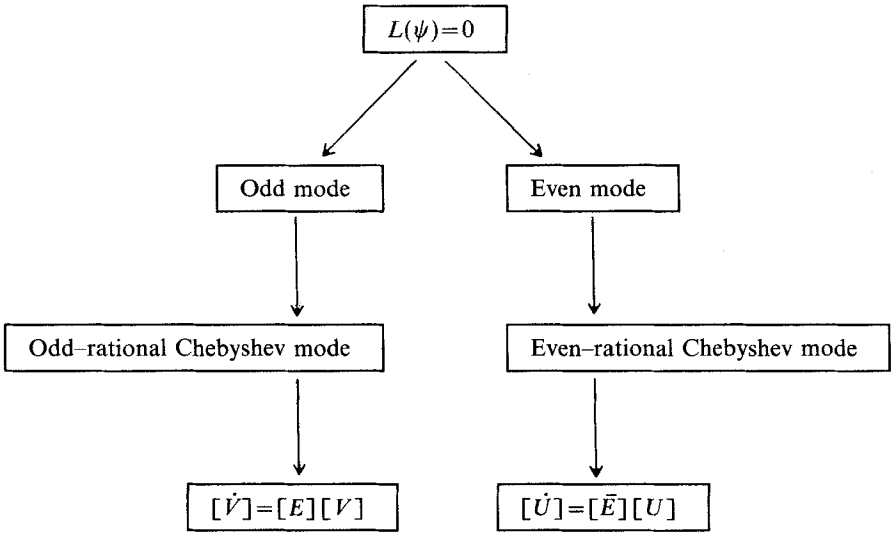

3.3. *Numerical method*

The salient features of our numerical procedures are briefly outlined here. More detail can be found in Chen.[34] By using the spectral Galerkin method in space twice, we reduce the governing equations of stability for the two independent modes into a system of ordinary differential equations in time. The problem becomes an initial value problem which is solved with appropriate initial conditions. The key of the formulation is to assure the correctness of formulation of the matrix and its submatrices with elements consisting of integrals. First the integrals involved in the matrices (14) and (15) are evaluated by the use of the Gauss quadrature, after the integration limits are transformed to 0 and π as explained earlier. The transformation of integrals are verified by *Mathematica*. The system of ODE given by (14) and (15) are solved by the use of ODEPACK provided at Cornell Theory Center. The number of terms retained in the orthogonal expansions are systematically increased until the desired accuracy is attained. For most of our computation, $M=10$ and $K=20$ are sufficient to guarantee the following criterion

$$\max \frac{|\psi_{K+1}-\psi_K|}{\psi_K} \leqslant \varepsilon,$$

where ε is chosen to be 0·0001 in all of the computation. Self-consistent test is conducted by letting $B=0$ for Kovaznay flow, we found the flow to be stable as expected. The code used here is similar to the one used in the study on stability of the Taylor vortex array.[35] One of the crucial tests of our code is to show monotonic decay of disturbance of Taylor vortex array at a parameter given by Lin and Tobak in energy stability of Taylor vortex array.

4. RESULTS AND DISCUSSION

Flow in laminar and turbulent wakes has been one of the leading problems in fluid mechanics and aerodynamics. A comprehensive experimental study can be found in Perry and Steiner[36] and direct numerical simulation by use of spectral element method is reported by Karniadakis and Triantaflyllou.[16] As Kovasznay mentioned, Kovasznay flow can be described as wake flow in the region $x>0$ behind a grid of wires. We can also imagine it as the flow passing an array of cylinders standing in the z-direction, while radius of cylinders are idealized like a mass particle in physics.

For full non-parallel flow stability theory, only a few of global stability analyses appear. To the author's knowledge, a general local stability analysis of genuine non-parallel flows has not yet appeared. An initial value problem approach to the Kovasznay flow gives us a chance to investigate the general local stability theory of genuine non-parallel flows. There are two parameters in Kovasznay flow: Reynolds number $\mathbb{R}$ and the flow parameter B which decides the length of wake flow. For Kovasznay flow, we would like to find at which $\mathbb{R}$ and B, the flow becomes unstable and what is next for the subsequent development for the flow.

4.1. Odd–rational Chebyshev mode

Figure 2 gives the time evolution of the disturbance with the initial state of odd mode prescribed by wavelength λ, amplitudes $A_1^1=0{\cdot}01$ and $A_2^1=-0{\cdot}01$ with the rest of A_m^k being zero. The basic state parameters are $\mathbb{R}=100$ and $B=5$. The spatial position chosen to observe the temporal evolution is $x=1/4$ and $z=1/4$. For this particular set of values of $(\mathbb{R}, B)$, the disturbance grows monotonically. This figure also serves to demonstrate the convergence of the method

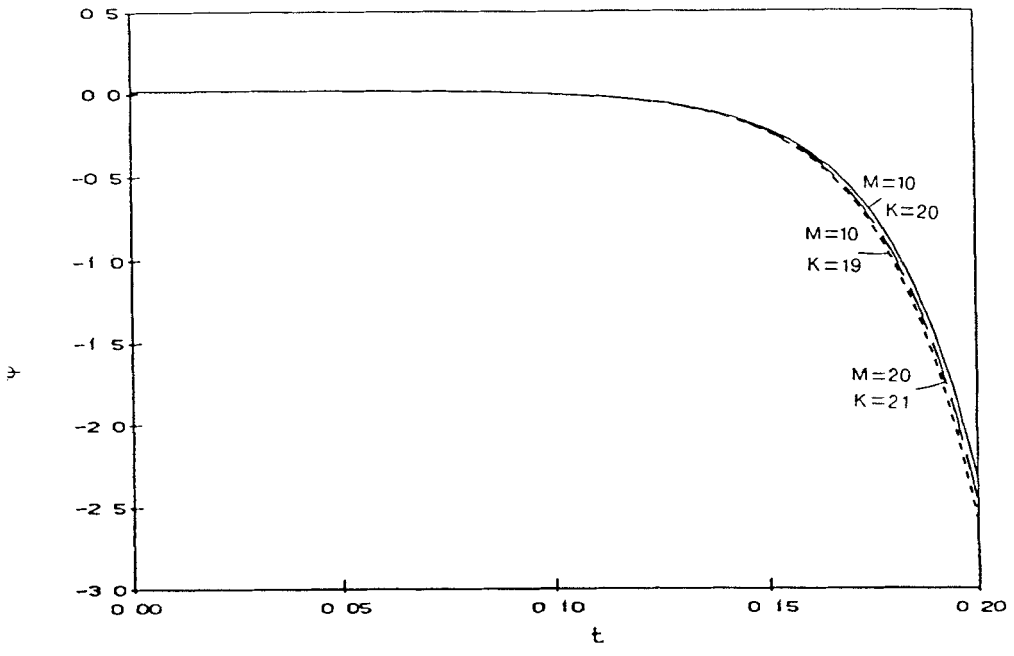

Figure 2. Convergence test. Odd–rational Chebyshev mode for $\mathbb{R}=100$, $B=5$, $A_1^1(0)=0{\cdot}01$, $A_1^1(0)=0{\cdot}01$. $A_1^2(0)=-0{\cdot}01$, at $x=z=1/4$, $\lambda=1$

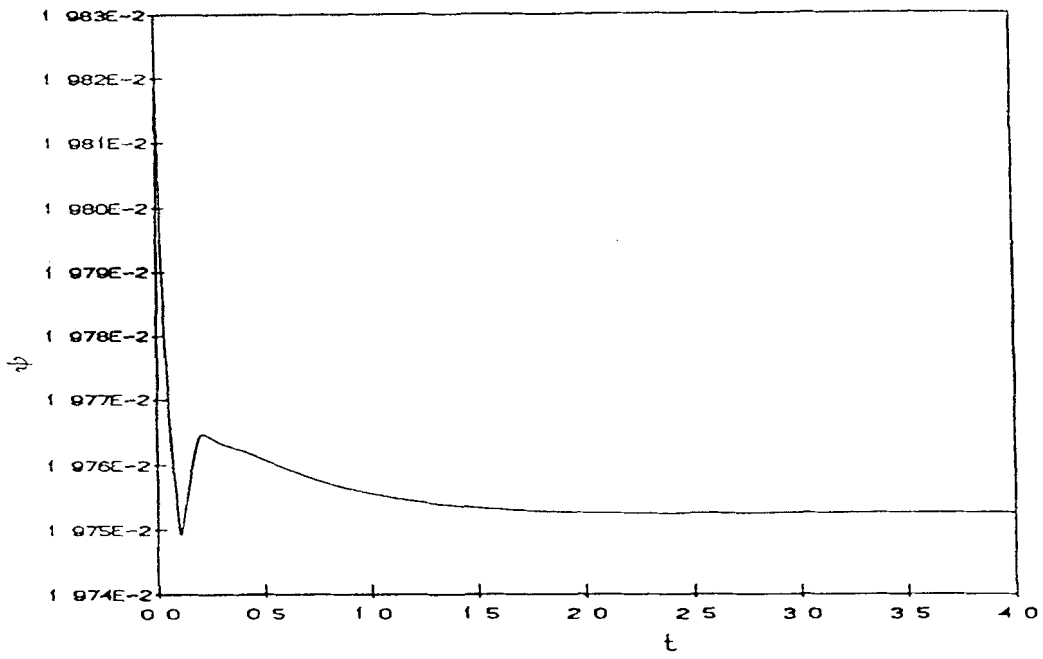

Figure 3. Stable odd-rational Chebyshev mode $\mathbb{R}=40$, $B=100$, $A_1^1(0)=0{\cdot}01$, $A_1^2(0)=-0{\cdot}01$, $x=z=1/4$, $\lambda=1$

of solution formulated in the previous section. Only three curves corresponding to three different numbers of terms retained are given in this figure for demonstration. Figure 3 shows that the disturbances decay and reach the equilibrium state at $\mathbb{R}=40$ and $B=100$. The flow keeps its original state in Figure 1.

When $\mathbb{R}=45$ and $B=25$, disturbances fluctuate with respect to time. When we increase B to 27·8, a wave pack propagation phenomena appears (Figure 4). Disturbances grow in such a way that a group of the so-called Carrier plane waves appear which are enclosed by a slowly varying envelope. Each envelope is bigger than the previous one and the flow becomes unstable. For $\mathbb{R}=45$ and $B=28$, disturbances oscillate and their envelope grows steadily with time (Figure 5). For $\mathbb{R}=45$ and $B=30$, wave pack propagation phenomena appear again (Figure 6). It is shown that, for a Reynolds number $\mathbb{R}$, there is a corresponding critical B at which disturbances start to grow and the flow becomes unstable. It is found that the larger the Reynolds number, the smaller the critical B becomes. The solution of the initial value problem described above yields a critical curve (Figure 7), in the $\mathbb{R}$–B plane, above which the flow is necessarily unstable with respect to the given initial disturbance. The flow is stable below the curve with respect to the same initial disturbance.

By using the energy method, Lin and Tobak[18] give a sufficient condition of global stability in the $\mathbb{R}$–B plane for Kovasznay flow. Their global bound curve is shown in Figure 8, with the critical curve obtained in the odd-rational Chebyshev mode here (note the log scale in vertical direction). Comparing the global stability results and the local stability results, we can see the conservative of the energy method with respect to odd–rational Chebyshev mode. However, there will be a better agreement for the even–rational Chebyshev mode described in the next section.

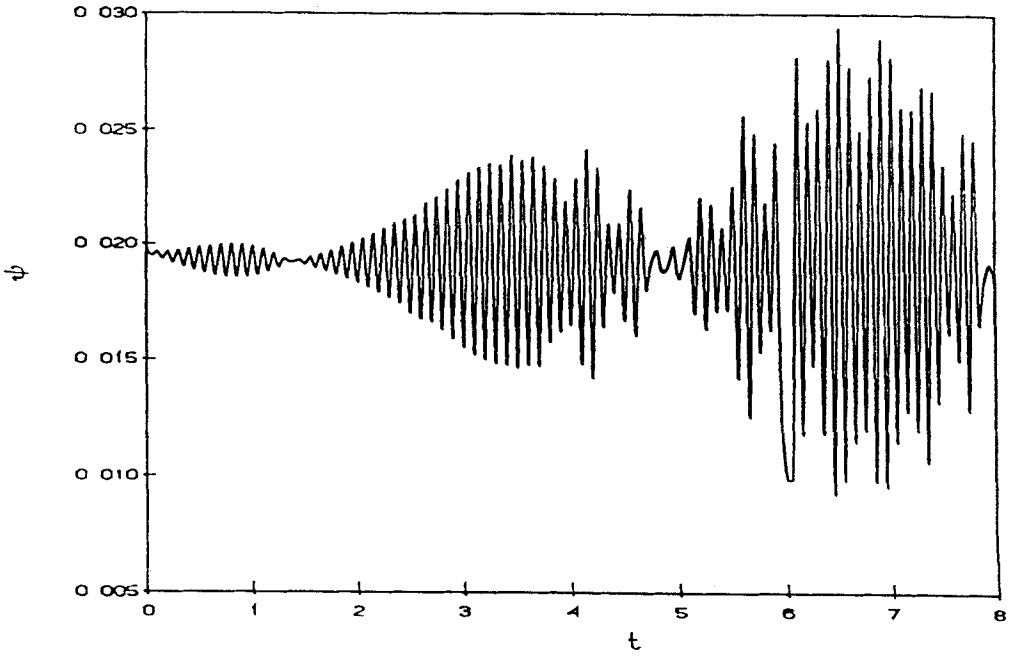

Figure 4. Oscillatory instability of odd-rational Chebyshev mode for $\mathbb{R}=45$, $B=27{\cdot}8$, $A_1^1(0)=0{\cdot}01$, $A_1^2(0)=-0{\cdot}01$, $x=z=1/4$, $\lambda=1$

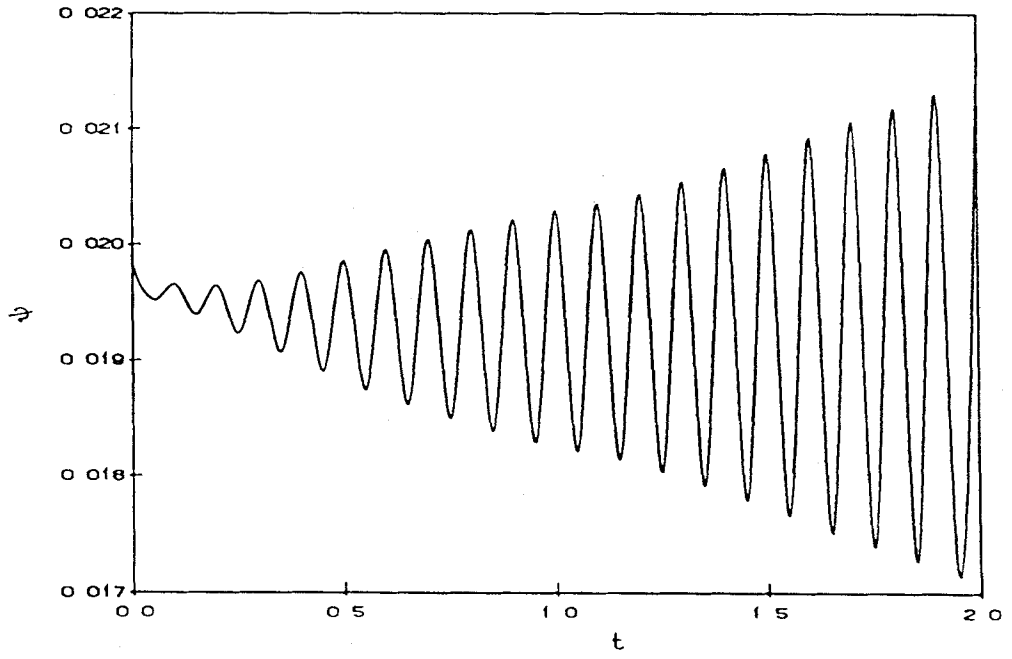

Figure 5. Oscillatory instability of odd-rational Chebyshev mode for $\mathbb{R}=45$, $B=28$, $A_1^1(0)=0{\cdot}01$, $A_1^2(0)=-0{\cdot}01$, $x=z=1/4$, $\lambda=1$

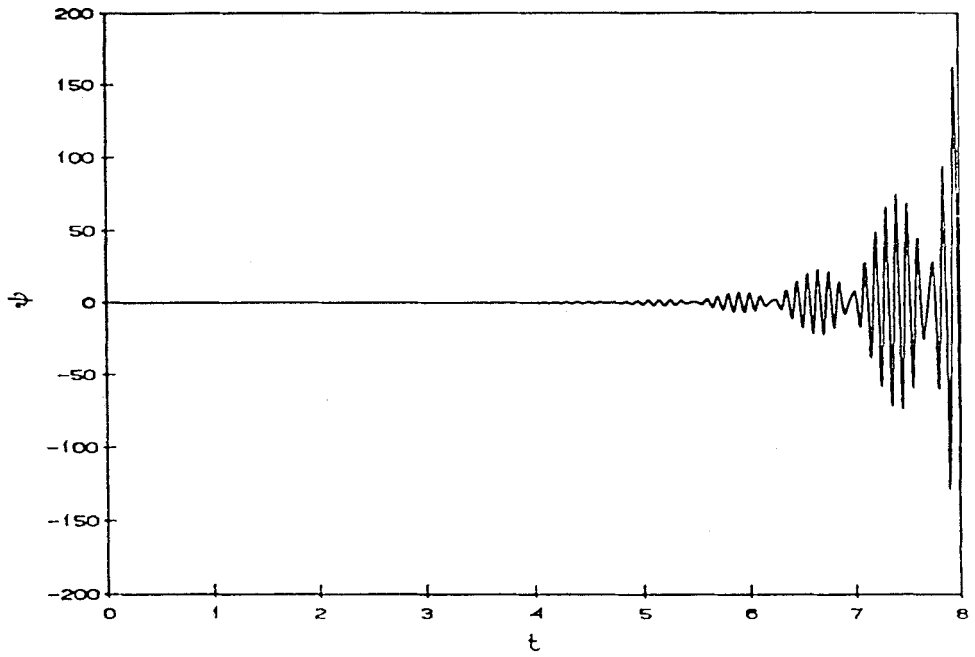

Figure 6. Oscillatory instability of odd-rational Chebyshev mode for $\mathbb{R}=45$, $B=30$, $A_1^1(0)=0{\cdot}01$, $A_1^2(0)=-0{\cdot}01$, at $x=z=1/4$, $\lambda=1$

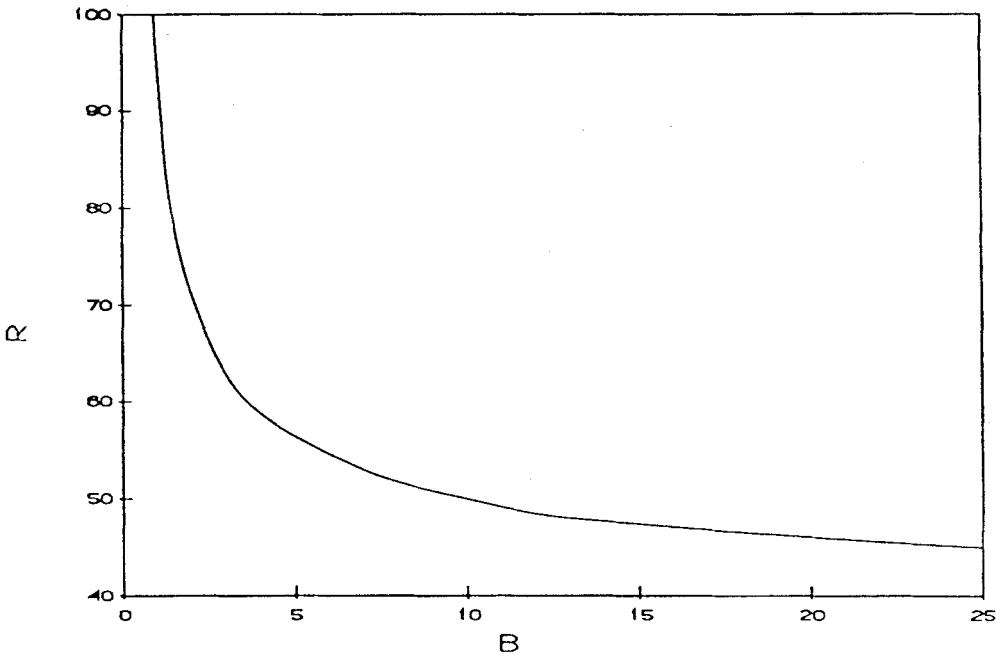

Figure 7. Critical curve of odd-rational Chebyshev mode for $A_1^1(0)=0{\cdot}01$, $A_1^2(0)=-0{\cdot}01$, at $x=z=1/4$, $\lambda=1$

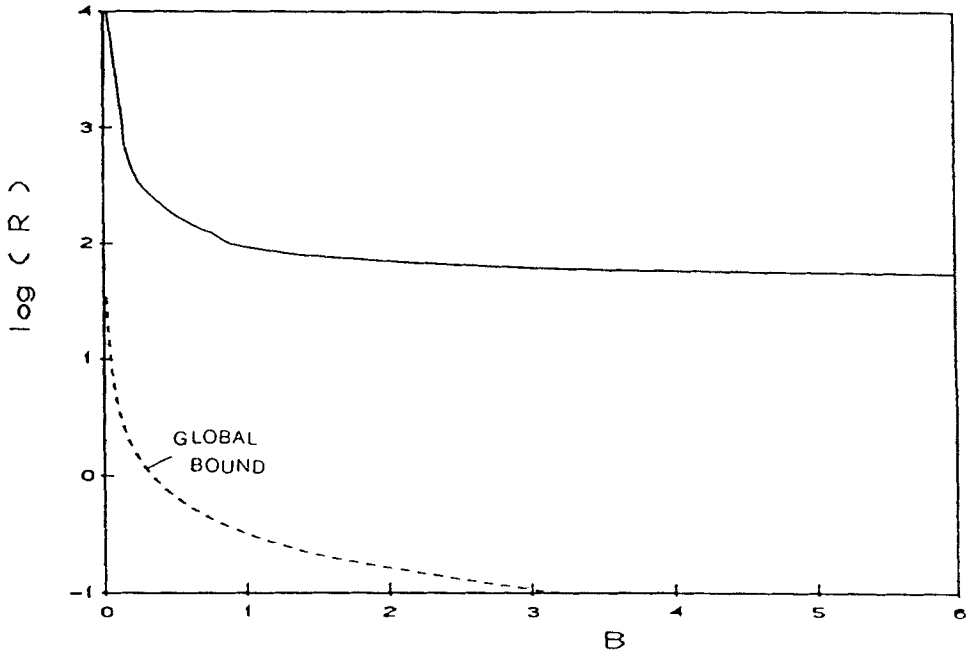

Figure 8. Comparison of local instability and global instability: — critical curve of odd-rational Chebyshev mode; —— bound of energy instability

From the contour plot of the perturbated flow ($\bar{\psi}+\psi$), we can vividly see how the flow becomes unstable through the vortex motion. For $\mathbb{R}=45$ and $B=27{\cdot}8$ (Figure 9a–f), disturbances start to affect the basic flow at $t=2{\cdot}5$. The stagnation points stretch first along the flow direction, and points continuously stretch until 'bubbles' appear downstream along the line of symmetry. As time goes on the bubbles, which are the vortex eddies, become progressively larger ($t=10{\cdot}4$, Figure 9a) until $t=11{\cdot}6$ (Figure 9b). The stagnation points are compressed by the flow from downstream. Moreover, big eddies become small eddies, and small eddies become smaller and smaller until they disappear. More bubbles appear elsewhere ($t=11{\cdot}6$). As time goes on, the eddies grow larger ($t=12{\cdot}6$, Figure 9c) until $t=13{\cdot}8$ (Figure 9d), the bigger eddies become small eddies again (Figure 9d). The smaller eddies will break further into point eddies and eddies elsewhere will grow until at certain stage, they will become small eddies (Figure 9e). The whole process consists of stagnation point oscillation stretched and compressed. The oscillation sustains throughout the process of big eddies becoming small eddies (large scale becomes small scale).

Figure 10a–d show the streamline pattern for $\mathbb{R}=45$ and $B=30$. The flow becomes unstable starting from the stagnation point which is compressed by the downstream (Figure 10a). The stagnation points stretch toward downstream and the eddies start to appear (Figure 10b). The eddies grow as the flow oscillates along the horizontal line at $t=2{\cdot}4$ eddies become bigger and the stagnation is compressed (Figure 10c). At $t=3{\cdot}0$ (Figure 10d), symmetrical vortex sheet forms and the flow arrives at a new flow structure. The onset of instability occurs through the oscillation of the stagnation point, from then on, the oscillation grows in time and spreads in space, eventually transitioning to the symmetric vortex street.

For $\mathbb{R}=50$ and $B=10{\cdot}0$ (Figures 11a–l), we can see from the streamline pattern that the flow becomes unstable starting from the stagnation points. As time goes on, more eddies are formed

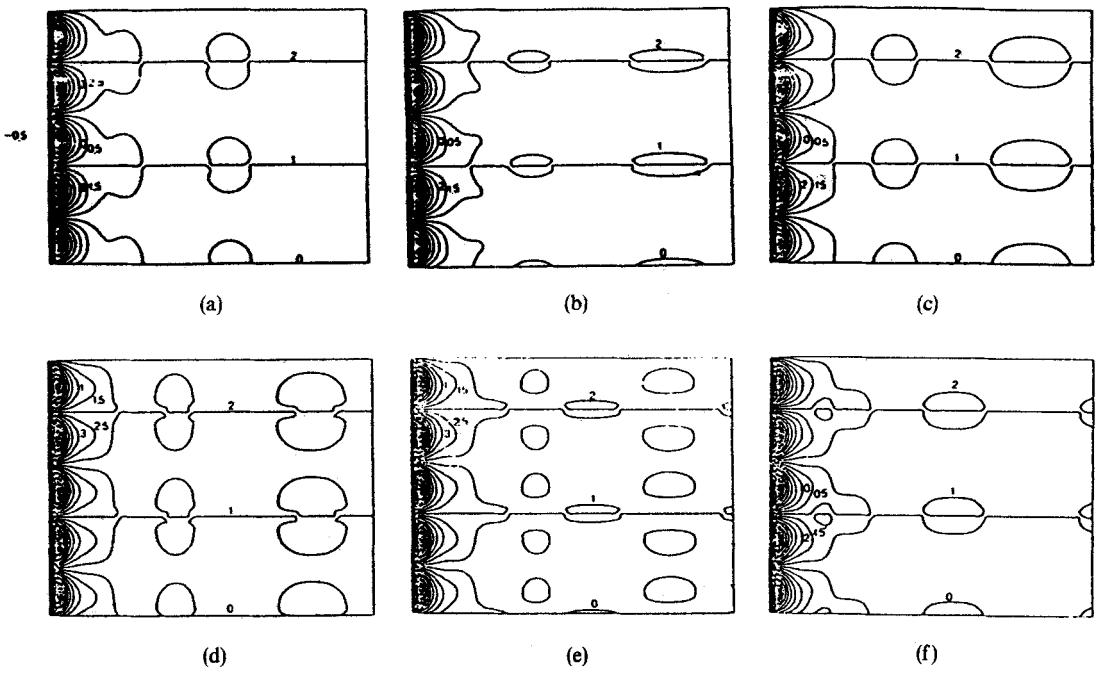

Figure 9. Streamline pattern of odd–rational Chebyshev mode for $\mathbb{R}=45$, $B=27{\cdot}8$; (*a*) $t=10{\cdot}4$; (*b*) $t=11{\cdot}6$; (c) $t=12.6$; (d) $t=13{\cdot}8$; (e) $t=14{\cdot}4$; (f) $t=15{\cdot}0$ and $0\leqslant x\leqslant 25$

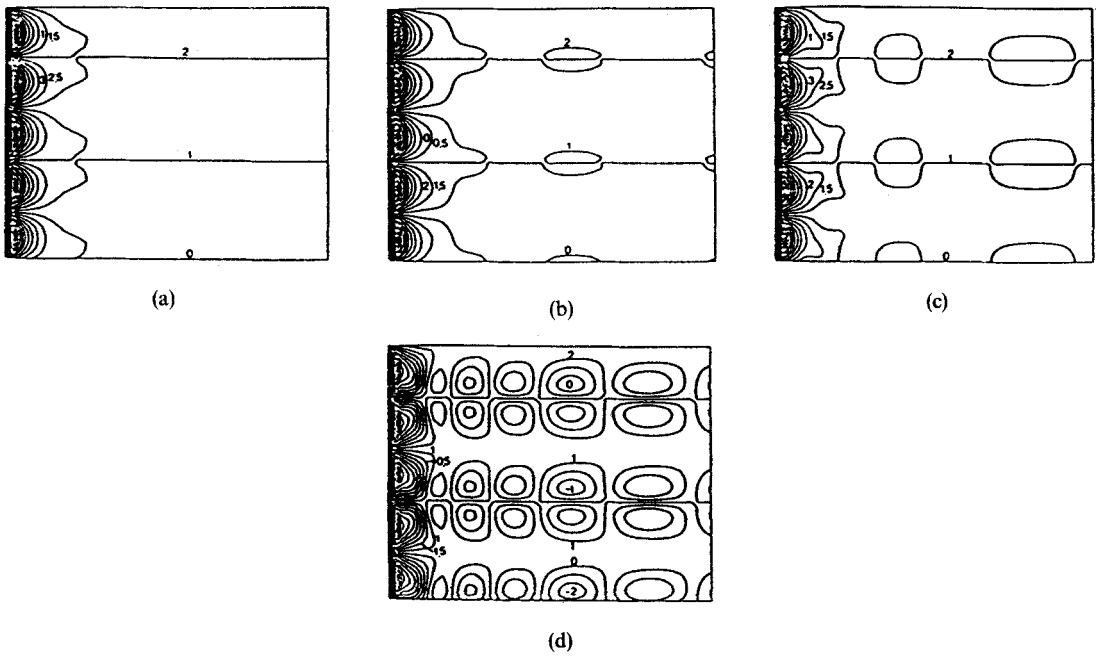

Figure 10. Streamline pattern of odd–rational Chebyshev mode for $\mathbb{R}=45$, $B=30$, at (a) $t=1{\cdot}2$; (b) $t=1{\cdot}8$; (c) $t=2{\cdot}4$; (d) $t=3{\cdot}0$ and $0\leqslant x\leqslant 25$

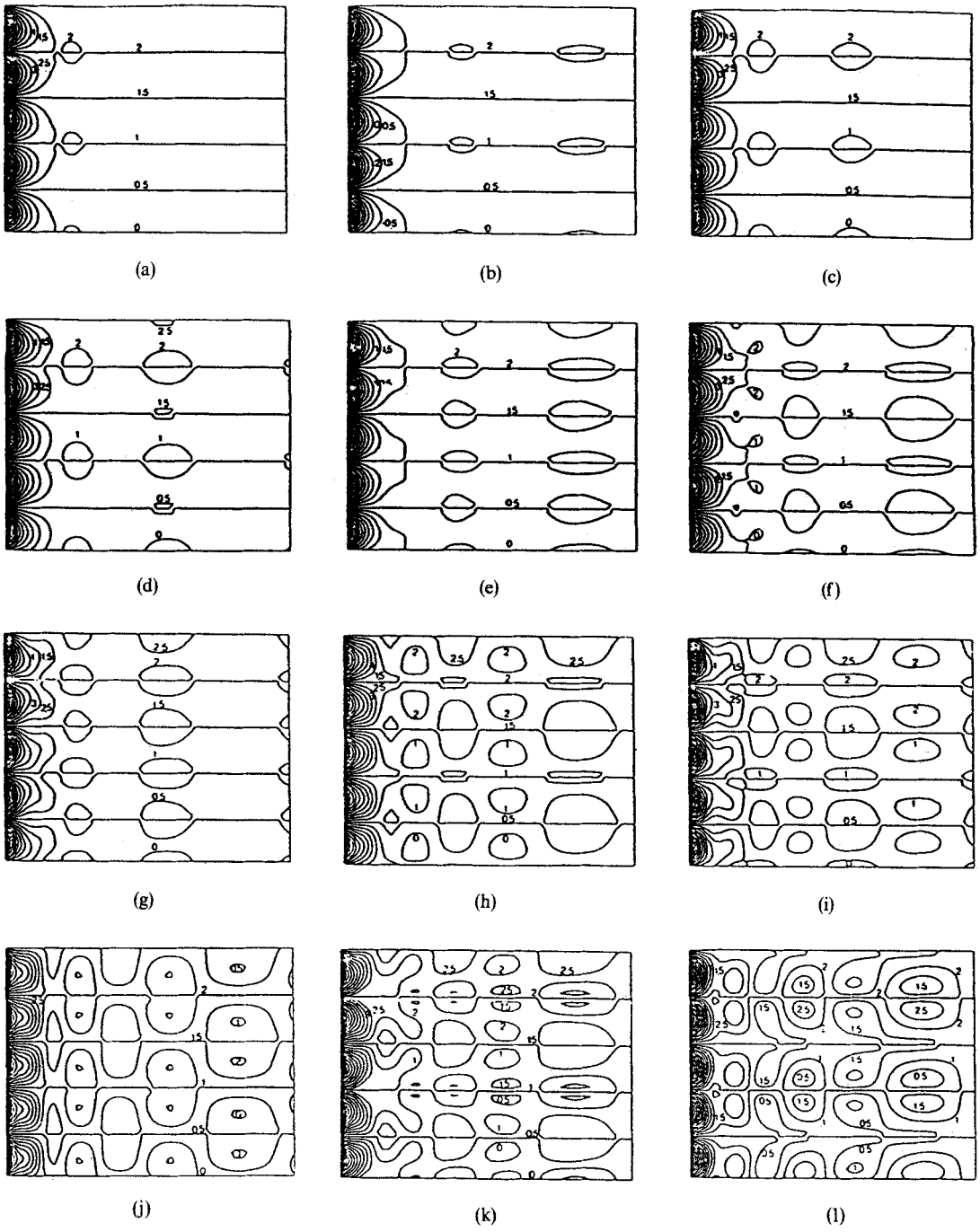

Figure 11. Streamline pattern of odd-rational Chebyshev mode for $\mathbb{R}=50$, $B=10$, (a) $t=8{\cdot}4$; (b) $t=9{\cdot}2$; (c) $t=10{\cdot}4$; (d) $t=12{\cdot}4$; (e) $t=13{\cdot}2$; (f) $t=15{\cdot}2$; (g) $t=16{\cdot}4$; (h) $t=17{\cdot}2$; (i) $t=18{\cdot}4$; (j) $t=19{\cdot}2$; (k) $t=19{\cdot}6$; (l) $t=20{\cdot}0$ and $0\leqslant x\leqslant 25$

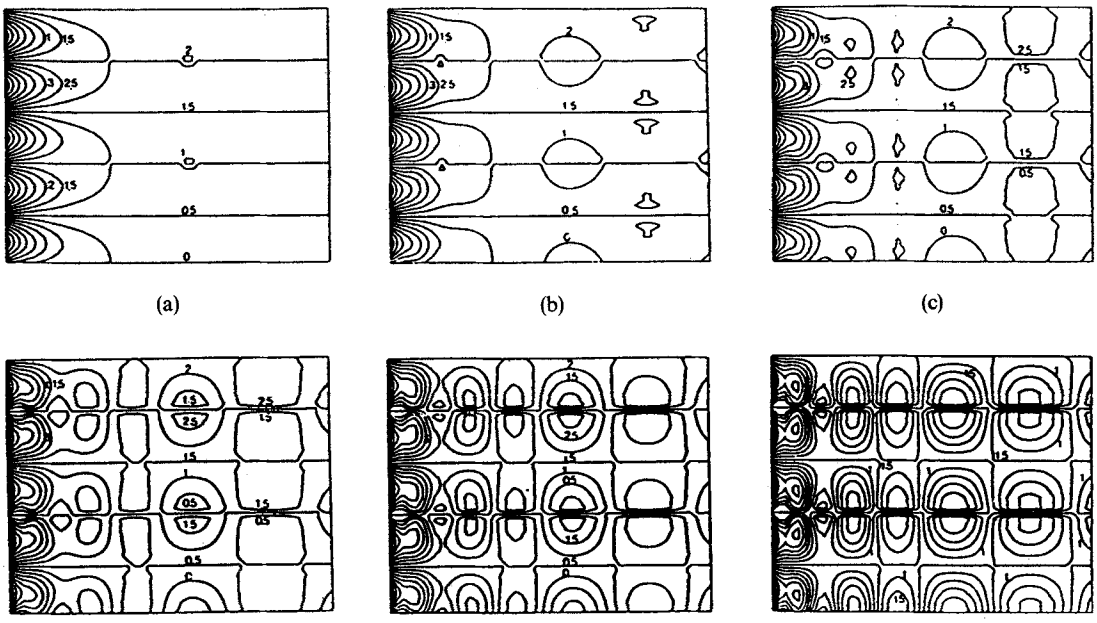

Figure 12. Streamline pattern of odd-rational Chebyshev mode for $\mathbb{R}=100$, $B=5$, (a) $t=0{\cdot}08$; (b) $t=0{\cdot}12$; (c) $t=0{\cdot}13$; (d) $t=0{\cdot}14$; (e) $t=0{\cdot}15$; (f) $t=0{\cdot}16$ and $0\leqslant x\leqslant 25$

along the downstream (Figure 11b–c) when they oscillate back and forth. This phenomenon is also observed by Ferré and Giralt[37] (Figures 10, 13, 14) who extract footprints of organized structures within a pattern recognition framework. At $t=16{\cdot}4$, big eddies start to break into small eddies (Figure 11f) and the eddies grow until they form a new configuration pattern: symmetrical vortex sheets. A fish-eye phenomenon is shown in Figure 11(l) in which we could imagine fish moving towards the upstream.

For $\mathbb{R}=100$ and $B=5$ (Figures 12a–f), instead of the onset of instability happening at the stagnation points, the flow first becomes unstable downstream. It is found that the stagnation points are more stable when $\mathbb{R}=100$ than in the case where $\mathbb{R}=50$. The outer configuration boundary of the attached eddies (like a half *Rankine ovoid* in aerodynamics) seems to be more stiff (Figures 12a and 12b). The small eddies are produced within the region of attached eddies without breaking the stagnation points (Figures 12c and 12d). As time goes on, inside eddies oscillate to break down the outer boundary of the attached eddies (*Rankine body*) at $t=0{\cdot}14$ (Figure 12e). In the whole process, the vortex motion dominates the flow field. The flow becomes a new configuration, a symmetrical vortex sheet structure exists behind each *Rankine ovoid* before turbulence develops.

It is found that longer the wavelength, the more unstable the flow will be. For $\mathbb{R}=45$, $B=27{\cdot}7$, we can see that disturbances oscillate and grow gradually for wavelength $\lambda=1$ (Figures 9a–e). When we increase λ from 1 to 2, we can see that disturbances grow very fast (Figure 13) and the flow becomes unstable earlier than the case when $\lambda=1$. The flow pattern for $\mathbb{R}=45$, $B=27{\cdot}8$, $\lambda=2$ can be seen in Figures (14a–e). Unlike the case for $\lambda=1$ at which if one stagnation point is compressed, the next one is also compressed and if one is stretched, the next one is also stretched (Figure 9a) at the same time. For $\lambda=2$, as we can see in Figures 14a–c, while one stagnation point

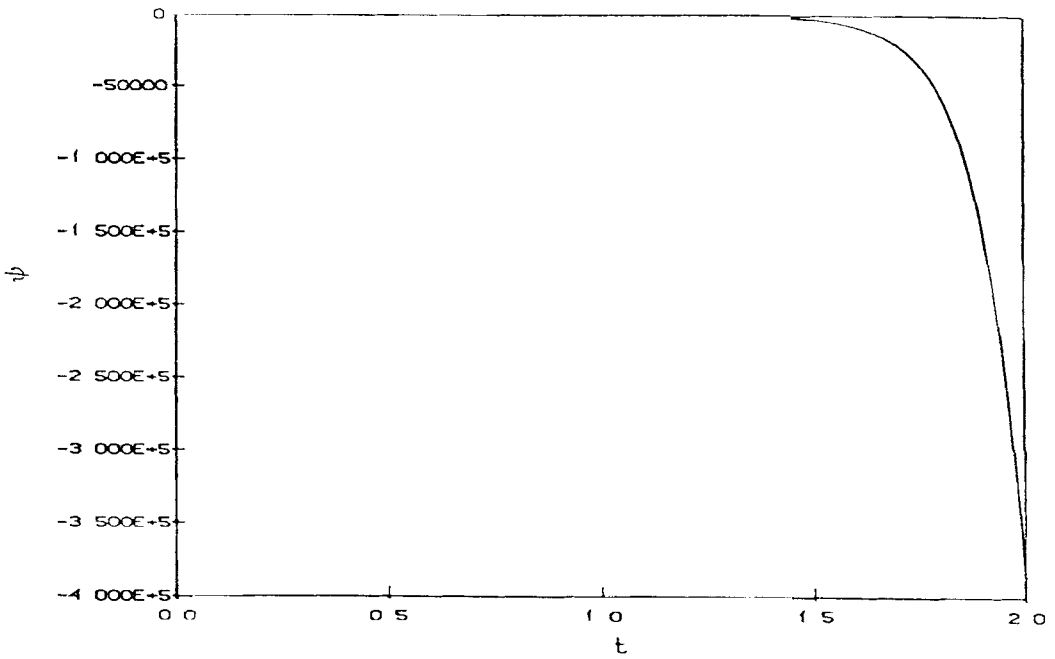

Figure 13. Wavelength effects for $\lambda = 2$, $\mathbb{R} = 45$, $B = 27{\cdot}8$, $A_1^1(0) = 0{\cdot}01$, $A_1^2(0) = -0{\cdot}01$, at $x = z = 1/4$

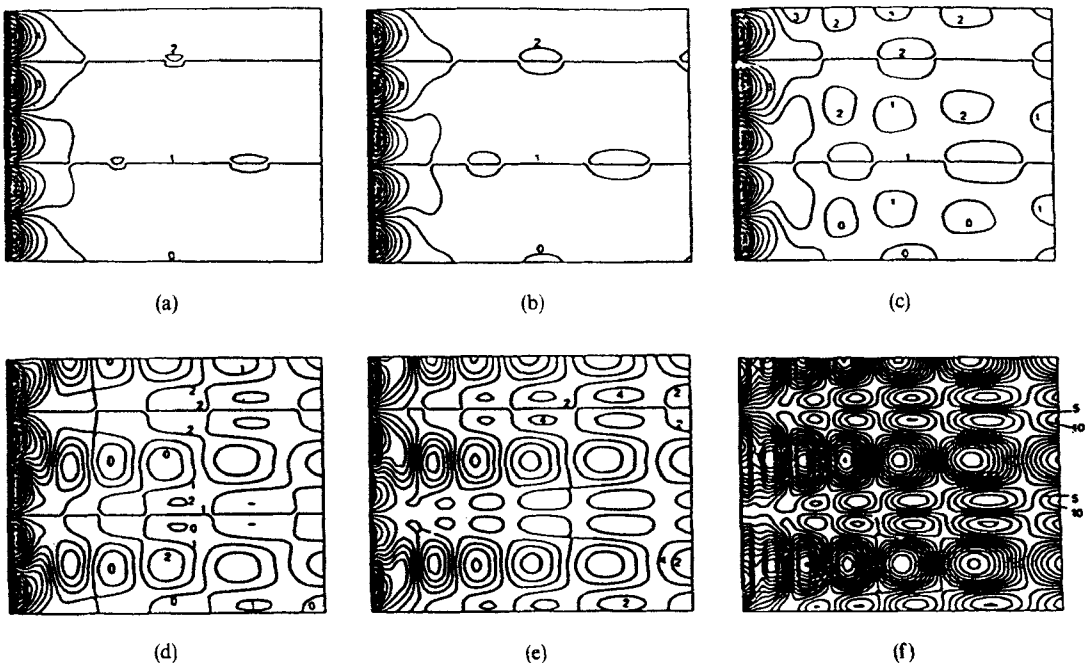

Figure 14. Streamline pattern of odd-rational Chebyshev mode for $\lambda = 2$, $\mathbb{R} = 45$, $B = 27{\cdot}8$, (a) $t = 0{\cdot}45$; (b) $t = 0{\cdot}495$; (c) $t = 0{\cdot}6$; (d) $t = 0{\cdot}7$; (e) $t = 0{\cdot}8$; (f) $t = 1{\cdot}0$ and $0 \leqslant x \leqslant 25$

is compressed, the next one is stretched. The attached eddies whose stagnation point is compressed, are compressed by the neighbouring attached eddies in the z-direction. The wavelength effects accelerate the interaction of eddies in the z-direction. The stagnation points finally disappeared as time went on under the effects of the wavelength. It is concluded that stagnation points are the most unstable locations if the wavelength is greater than 1.

4.2. *Even–rational Chebyshev mode*

Carrying the inner products of the governing equation with an even function in the z-direction and the rational Chebyshev function in the x-direction, we have the even–rational Chebyshev mode. Following a similar process to what we have done in the odd–rational Chebyshev mode, we have found the critical curve and streamline patterns for even–rational Chebyshev mode.

It is found that the flow becomes more unstable corresponding to the lower Reynolds number and B in the even–rational Chebyshev mode than that in the odd–rational Chebyshev mode as can be seen in the critical curve in Figure 15. The results obtained here are more closed to the global stability results than odd–rational Chebyshev mode. So the even–rational Chebyshev mode which is corresponding to antisymmetric disturbances is more unstable than the odd–rational Chebyshev mode which is corresponding to symmetric disturbances. The reason is that the basic flow has an odd function structure in the z-direction.

By comparing the critical curve with the global results, it is shown that the critical curve of the even–rational Chebyshev mode is much closer to the global bound given by Lin and Tobak than that of the odd–rational Chebyshev mode (we do not need a log scale in vertical axis).

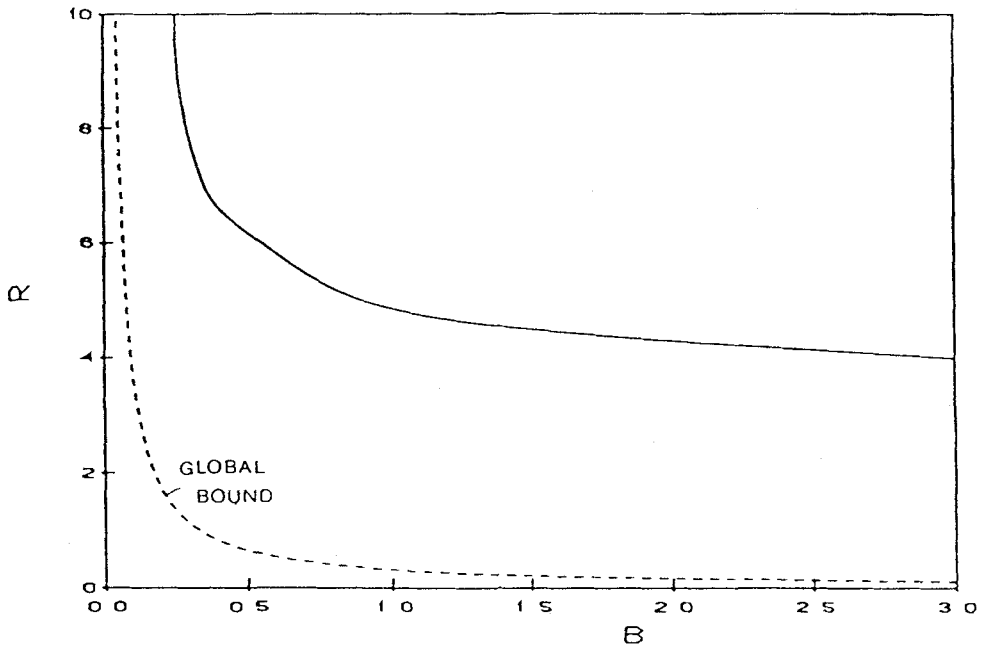

Figure 15. Comparison of local instability and global instability: ——critical curve of even–rational Chebyshev mode; —— bound of energy instability

Unlike the odd–rational Chebyshev mode in which the flow pattern has a symmetric vortex structure, the even–rational Chebyshev mode has formed an unsymmetrical vortex sheet configuration: Kármán vortex street. By studying the flow passing a cylinder, Von Kármán discovered that the wake behind the cylinder becomes unstable in such a way that oscillations in the wake grow in amplitude and, finally, roll up into discrete, unsymmetrical vortices with a very regular spacing. This trail of vortices in the wake is known as the Kármán vortex street.

It is shown that the Kovasznay flow possesses the Kármán vortex street phenomena when subjected to the even–rational Chebyshev mode perturbation. For $\mathbb{R}=7$ and $B=0{\cdot}4$, Figures (16a–f), the length of the attached eddies is much smaller here than the case of bigger $\mathbb{R}$ and B ($l=0{\cdot}2496$). So we enlarge the bounded eddies region for $0<x<2$. We can see that symmetrical attached eddies become unsymmetrical attached eddies (Figure 16c). At $t=4{\cdot}0$, the flow starts to oscillate behind each attached eddy. To observe further downstream of the wake in the Kovasznay flow, we plot the flow field for $0\leqslant x\leqslant 25$ (Figures 17a–f). As time goes on, oscillations in the Kovasznay flow grow in amplitude and gradually roll up into unsymmetrical vortices. The vortex sheet forms closer to the upstream. As one goes further downstream, the vortex sheets develop spatially (Figure 17f). Further downstream, the formed vortex is bigger than the one upstream. The vortices become stronger and stronger and become a new flow pattern before turbulence develops. Moreover, the Kovasznay flow possesses many vortex sheets periodically in the z-direction, as the characteristic of the basic flow. Similar phenomena can be found for $\mathbb{R}=10$ and $B=0{\cdot}25$ in Figures 18a–f.

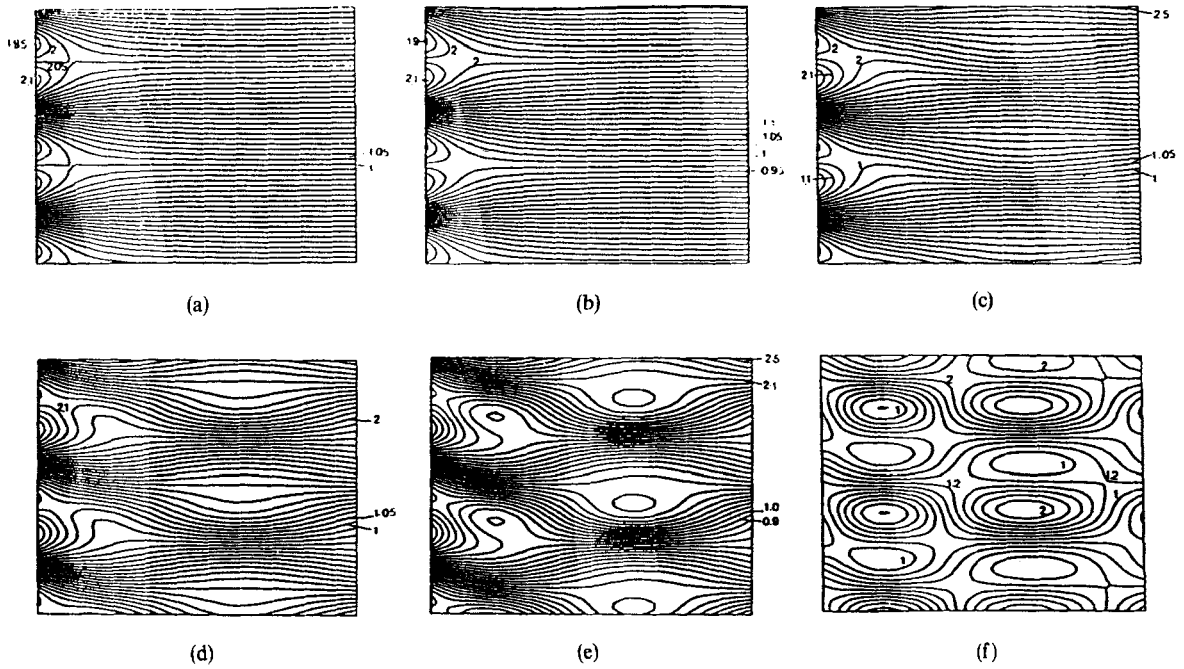

Figure 16. Streamline pattern of even–rational Chebyshev mode for $0\leqslant x\leqslant 2$, $\lambda=1$, $\mathbb{R}=7$, $B=0{\cdot}4$, at (a) $t=0{\cdot}0$; (b) $t=0{\cdot}8$; (c) $t=3{\cdot}2$; (d) $t=4{\cdot}0$; (e) $t=4{\cdot}5$; (f) $t=6{\cdot}0$

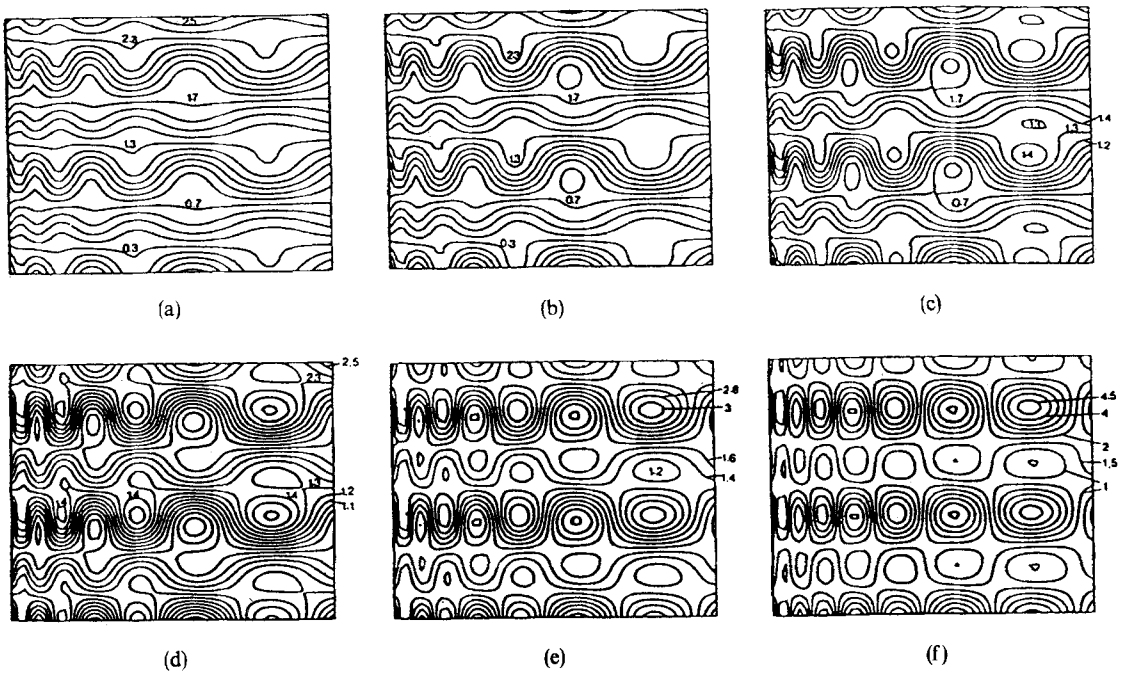

Figure 17. Streamline pattern of even–rational Chebyshev mode for $0 \leqslant x \leqslant 25$, $\lambda = 1$, $\mathbb{R} = 7$, $B = 0{\cdot}4$, at (a) $t = 3{\cdot}6$; (b) $t = 3{\cdot}9$; (c) $t = 4{\cdot}2$; (d) $t = 4{\cdot}5$; (e) $t = 5{\cdot}1$; (f) $t = 6{\cdot}0$

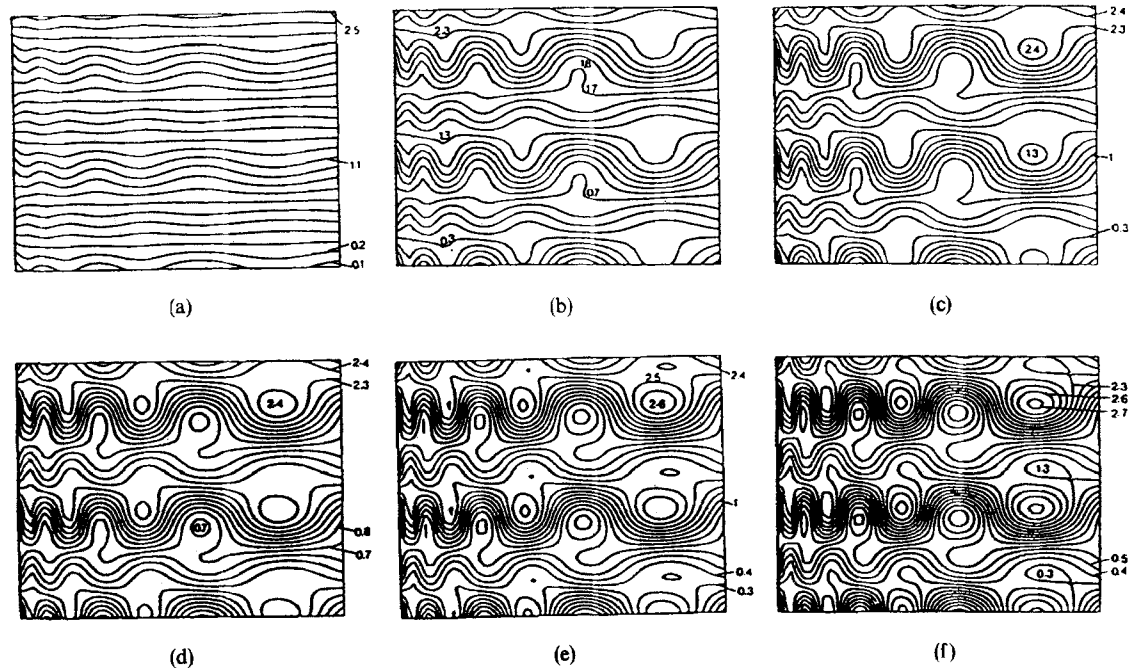

Figure 18. Streamline pattern of even–rational Chebyshev mode for $0 \leqslant x \leqslant 25$, $\lambda = 1$, $\mathbb{R} = 10$, $B = 0{\cdot}25$, at (a) $t = 6{\cdot}0$; (b) $t = 9{\cdot}6$; (c) $t = 10{\cdot}5$; (d) $t = 10{\cdot}8$; (e) $t = 11{\cdot}4$; (f) $t = 12{\cdot}0$

5. CONCLUSIONS

The Kovasznay flow becomes unstable and the flow develops into new configuration patterns: symmetrical vortex street and unsymmetrical vortex street which resembles Kármán vortex street. While oscillation motions sustain through vortex birth and break down in certain parameters in odd Fourier mode, monotonic growth of the disturbance is shown in even Fourier mode which corresponds to antisymmetric disturbances.

The Kovasznay flow is found to be more unstable with respect to the even Fourier mode of the perturbation stream function. This explains why the Kármán vortex street is observed in the experiment instead of symmetrical vortex street. The advantage of linear theory is the decoupling of the odd mode and even mode. The present work is limited by the fact that theory is linear. Nevertheless, it is hoped that the stretching of the linear theory will allow us to gain some physical insights into non-parallel stability. However, as Herbert[2] remarked, the extension of the stability theory of parallel flow could be realized either by non-parallelism or by non-linearity, but not both. The present study attacked one of the two important aspects: non-parallelism. Non-linearity will lead us to a turbulence region instead of onset of instability, which is the main task of the linear stability. The coherent structure and chaotic state of the flow can be pursued by a dynamic system study. The dynamic system for Kovasznay flow can be obtained by adding non-linear terms corresponding to the convective acceleration terms in Navier–Stokes equations and forms a similar system to (14). Based on this system, one may investigate the large time evolution of unstable Kovasznay flow and extract information concerning the possible coherent chaotic structure in the wake.

Through the course of the investigation, on the basis of the existing evidence, we have found several general characteristics of the non-parallel flow stability.

Vortex motion. Vortex birth, growth and merger play a key role in the non-parallel flow instability. Onset of instability accompanies the birth of vorticity. Vorticity exists before turbulence develops.

No normal mode approach (both spatial and temporal). For Kovasznay flow, non-parallelism and unbounded domain prevents us from finding unique eigenvalues, both spatial and temporal. This is concluded based on our investigation as well as the existing evidence. Consequently, no traditional neutral curve exists in the non-parallel flow. Moreover, terms like absolute and convective stability are avoided due to this characteristic. Since we do not have spatial eigenvalues and temporal eigenmodes to distinguish the definition initiated by plasma physicist.

Experiment propose. No experiment for Kovasznay flow appeared so far based on author's knowledge. It will be a very good physical mode to do the experiment. Since the basic state is an exact solution of Navier–Stokes equation, experimentalists are invited to do the experiment in order to get more physical insight of full non-parallel flows.

ACKNOWLEDGEMENTS

I thank Prof. S. P. Lin for his initiation of the problem and guidance. I have benefitted from a conversation with Prof. G. K. Batchelor at Clarkson Inn concerning the eigenvalue problem. I thank Prof. Prosperetti for kindly providing me with his early work on Kovasznay flow. The computation was carried out with the computer facility at Clarkson University and with the Cornell National Super-computer Facility which is funded by the NSF, the State of New York, and the IBM Corporation.

REFERENCES

1. J. T. Stuart, 'Nonlinear stability theory', *Ann. Rev. Fluid Mech.*, **3**, 347–370 (1971).
2. T. Herbert, 'Appearance of transition in boundary layers', *Newport 1989 Conf. on Turbulence*, Newport, RI, 1989.
3. T. Tatsumi and T. Kakutani, 'The stability of a two-dimensional laminar jet', *J. Fluid Mech.*, **4**, 261 (1958).
4. H. Lanchon and W. Eckhaus, 'Sur l'analyse de la stabilité des écoulements faiblement divergents', *J. de Mécanique*, **3**(4), 446–459 (1964).
5. M. Bouthier, 'Stabilité Linéaire des écoulements presque paralléles', *J. de Mécanique*, **11**(4), 599–621 (1972).
6. C. H. Ling and W. C. Reynolds, 'Non-parallel flow corrections for the stability of shear flows', *J. Fluid Mech.*, **59**, 571–591 (1973).
7. M. Gaster, 'On the effects of boundary-layer growth of flow stability', *J. Fluid Mech.*, **66**, 465–480 (1974).
8. W. S. Saric and A. H. Nayfeh, 'Nonparallel stability of boundary-layer flows', *Phys. Fluids*, **18** (1975)
9. F. T. Smith, 'Nonlinear stability of boundary layers for disturbances of various sizes', *Proc. Roy. Soc.*, **A368**, 573–589 (1980).
10. P. Hall, 'Taylor–Gövtler vortices in fully developed or boundary layer flows', *J. Fluid Mech.*, **124**, 475–494 (1982).
11. P. Hall, 'Linear development of Görtler vortices in growing boundary layers', *J. Fluid Mech.*, **130**, 41–58 (1983).
12. W. Asrar and A. H. Nayfeh, 'Nonparallel stability of heated two-dimensional boundary layers', *Phys. Fluids*, **28**, 1263–1272 (1985).
13. S. Wakitani, 'Non-parallel flow stability of a two-dimensional buoyant plume', *J. Fluid Mech.*, **159**, 241–258 (1985).
14. K. Gotoh, M. Yamada and J. Mizushima, 'The theory of stability of spatially periodic parallel flows', *J. Fluid Mech.*, **127**, 45–58 (1983).
15. J. M. Chomaz, P. Huerre and L. G. Redekopp, Bifurcations to local and global modes in spatially developing flows', *Phys. Rev. Lett.*, **60**(1), 25–28 (1988).
16. G. E. Karniadakis and G. S. Triantaflyllou, 'Frequency section and asymptotic states in laminar wakes', *J. Fluid Mech.*, **199**, 441 (1989).
17. S. P. Lin and M. Tobak 'Spectral stability of Taylor's vortex array', *Phys. Fluids*, **29**, 3477 (1986).
18. S. P. Lin and M. Tobak, 'Nonlinear stability of a flow with bound eddies', *Phys. Fluids*, **30**, 3388–3390 (1987).
19. V. Coscia, 'Nonlinear stability of a laminar flow past a two-dimensional grid', *Phys. Fluids*, **A1**, 1747–1749 (1989).
20. P. G. Drazin and W. H. Reid, *Hydrodynamic Stability*, Cambridge University Press, Cambridge, 1981.
21. G. I. Taylor, 'On the decay of vortices in a viscous fluid", *Phil. Mag.*, **46**, 671–674 (1923).
22. L. S. G. Kovasznay, 'Laminar flow behind a two-dimensional grid', *Proc. Camb. Phil. Soc.*, **44**, 58 (1948).
23. D. N. Beaumont, 'The stability of spatially periodic flows', *J. Fluid Mech.*, **108**, 461–471 (1980)
24. A. Prosperetti, 'Laminar flow at large distances from an infinite two-dimensional grid', *J. de Mécanique* **15**(2) (1976).
25. R. R. Lagnado, N. Phan-Thien and L. G. Leal, 'The stability of two-dimensional linear flow', *Phys. Fluids*, **27**, 1094–1101 (1984).
26. C. E. Grosch and H. Salwen, 'The continuous spectrum of the Orr–Sommerfeld equation. Part 1. The spectrum and the eigenfunctions', *J. Fluid Mech.*, **87**, 33–54 (1978).
27. A. D. D. Craik, *Wave Interactions and Fluid Flows*, Cambridge University Press, Cambridge, 1985.
28. G. K. Batchelor, 'The stability of a large gas bubble rising through liquid', *J. Fluid Mech.*, **184**, 399–422 (1987).
29. K. K. Tung, 'Initial-value problems for Rossby wave in a shear flow with critical layer', *J. Fluid Mech.*, **13**, 443–469 (1983).
30. F. Carrier and C. T. Chang, 'On an initial value problem concerning Taylor instability of incompressible fluids', *Quart. Appl. Math.*, **16**, 436–439 (1959).
31. L. D. Landau and E. M. Lifshitz, *Fluid Mechanics*, Pergamon Press, London, 1959
32. J. P. Boyd, 'Orthogonal rational functions on a semi-infinite interval', *J. Comput. Phys.*, **70**(1), 63–88 (1987).
33. S. A. Orszag, 'Galerkin approximation to flow within slabs, spheres and cylinders', *Phys. Rev. Lett.*, **18**, 1100–1103 (1971).
34. H. B. Chen, 'On the linear and nonlinear stability of non-parallel flow', *Ph.D. Thesis*, Clarkson University, 1989.
35. S. P. Lin and H. B. Chen, 'Instability of Taylor's vortex array'. *Proc. Roy. Soc.* (communication with J. T. Stuart) (submitted).
36. A. E. Perry and T. R. Steiner, 'Large-scale vortex structures in turbulent wakes behind bluff bodies. Part 1. Vortex formation processes', *J. Fluid Mech.*, **174**, 233–270 (1987).
37. J. A. Ferré and F. Giralt, 'Pattern-recognition analysis of the velocity field in plane turbulent wakes', *J. Fluid Mech.*, **198**, 27–64 (1989).
38. G. K. Batchelor, *An Introduction to Fluid Dynamics*, Cambridge University Press, Cambridge, 1967.
39. G. K. Batchelor, 'A new theory of the instability of a uniform fluidized bed', *J. Fluid Mech.*, **193**, 75–110 (1988).
40. B. Bayly, S. A. Orszag and T. Herbert, 'Instability mechanisms in shear-flow transition', *Ann. Rev. Fluid Mech.*, **20**, 359–391 (1988).
41. J. Bennett and P. Hall, 'On the secondary instability of Taylor–Gortler vortices to Tollmein–Schlichting waves in fully developed flows', *J. Fluid Mech.*, **186**, 445–469 (1988).
42. J. P. Boyd, Complex coordinate methods for hydrodynamic instabilities and Sturm–Liouville eigenproblems with an interior singularity', *J. Comput. Phys.*, **57**, 453–471 (1985).
43. B. J. Cantwell, 'Organized motion in turbulent flow', *Ann Rev. Fluid Mech.*, **13**, 457–515 (1986).
44. C. Canuto, M. Y. Hussaini, A. Quarteroni and T. A. Zang, *Spectral Methods in Fluid Dynamics*, Springer, Berlin, 1987.

45. H. B. Chen, S. P. Lin, A. Lahbabi and H. C. Chang, 'Linear and nonlinear stability of two exact periodic nonparallel flows', Manuscript, 1991.
46. R. J. Deissler, 'Spatially growing waves, intermittency, and convective chaos in an open-flow system', *Physica D*, **25D,** 233–260 (1986).
47. R. C. DiPrima and J. T. Stuart, 'Hydrodynamic stability', *J. Appl. Mech.*, **50,** 983–991 (1983).
48. W. Eckhaus, *Studies in Non-Linear Stability Theory*, Springer, Berlin, 1965.
49. B. A. Finlayson, *The Method of Weighted Residuals and Variational Principles: with Application in Fluid Mechanics, Heat and Mass Transfer*, Academic Press, New York, 1972.
50. C. A. J. Fletcher, *Computational Galerkin Methods*, Springer, New York 1984.
51. M. Gaster, 'The development of a two-dimensional wavepacket in a growing boundary layer', *Proc. R. Soc. Lond.* **A384,** 317–332 (1982)
52. D. Gottlieb and S. A. Orszag, *Numerical Analysis of Spectral Method: Theory and Applications*, SIAM-CBMS, Philadelphia, 1977.
53. P. Hall and F. T. Smith, 'On the effects of non-parallelism, three-dimensionality, and mode interaction in nonlinear boundary-layer stability', *Stud. Appl. Math.*, **70,** 91–120 (1984).
54. P. Hall, 'The nonlinear development of Gortler vortices in growing boundary layers', *J. Fluid Mech.*, **193,** 243–266 (1988).
55. T. Herbert, 'Secondary instability of boundary layers', *Ann. Rev. Fluid Mech.*, **20,** 487–526 (1988).
56. C. C. Lin, 'On the stability of two-dimensional parallel flows', *Quart. Appl. Math.*, **3,** 117–42, 218–234 and 277–301 (1945).
57. C. C. Lin, *The Theory of Hydrodynamic Stability*, Cambridge University Press, Cambridge, 1955.
58. C. C. Lin and L. A. Segel, *Mathematics Applied to Deterministic Problems in the Natural Sciences*, Macmillan, New York, 1974.
59. L. Lin, 'Numerical simulation of the onset of transition of a nonparallel flow', *M.S. Thesis*, Clarkson University, Clarkson, 1987.
60. S. P. Lin, H. B. Chen and M. Tobak, 'Instability of a nonparallel flow', *Proc. 1st Int. Conf. of Fluid Mechanics*, Beijing, 1987.
61. S. P. Lin, H. B. Chen and M. Tobak, 'Nonlinear stability of a reversed flow over a flat plate with suction', *Proc. Symp. in honor of C. C. Lin*, MIT Press Cambridge, World Scientific, 1987, p. 164
62. A. H. Nayfeh and N. M. El-Hady, 'Nonparallel stability of two-dimensional nonuniformly heated boundary-layers flows', *Phys. Fluids*, **23** (1980).
63. A. H. Nayfeh and A. Al-Maaitah, 'Influence of streamwise vortices on Tollmien–Schlichting waves', *Phys. Fluids.*, **31** (1988).
64. S. A. Orszag, 'Numerical methods for the simulation of turbulence. Sommerfeld equation', *Phys. Fluids*, **12,** 250–257 (1969).
65. S. A. Orszag, 'Spectral methods for problems in complex geometries', *J. Comput. Phys.*, **37,** 70–92 (1980).
66. R. T. Pierrehumbert and S. E. Widnall, 'The two- and three-dimensional instabilities of a spatially periodic shear layer', *J. Fluid Mech.*, **114,** 59–82 (1982).
67. H. Reed and W. S. Sarice, 'Stability of three-dimensional boundary layers', *Ann. Rev. Fluid Mech.*, **21,** 235–284 (1989).
68. F. T. Smith, 'On the non-parallel flow stability of the Blasius boundary layer', *Proc. Roy. Soc.*, **A366,** 91–109 (1979).
69. J. T. Stuart, 'Hydrodynamic stability', in L. Rosenhead (ed.), *Laminar Boundary Layer*, Clarendon Press, Oxford, 1963, pp. 492–579.
70. J. T. Stuart, 'Instability of laminar flows, nonlinear growth of fluctuations and transition to turbulence', in L. Tatsumi (ed.), *Turbulence and Chaotic Phenomena in Fluids*, IUTAM, 1984.
71. H. L. Swinney and J. P. Gollub, *Hydrodynamic Instabilities and The Transition to Turbulence*, Springer, Berlin, 1981.
72. G. S. Triantaflyllou, K. Kupfer and Bers, A. 'Absolute instabilities and self-sustained oscillations in the wake of circular cylinders', *Phys. Rev. Lett.*, **59,** 1914–1917 (1987).
73. J. M. T. Thompson and H. B. Stewart, *Nonlinear Dynamics and Chaos*, Wiley, New York, 1986.
74. D. T. Valentine and A. G. Mohamed, 'High-order Navier–Stokes equations solver and a new test problem', *Bullet. APS*, **33,** 2265 (1988).
75. X. Yu and J. T. C. Liu, 'On the secondary instability in the transition Process in wall bounded shear flow', Bulletin in American Physical Society Division of Fluid Dynamics 43rd Annual Meeting, Cornell University, Ithaca, New York; *Proc. R. Soc. Lond.* **A381,** 407–418 (1989).
76. R. L. Zollars and W. B. Krantz, 'Non-parallel flow effects of the stability of film flow down a right circular cone', *J. Fluid Mech.*, **96,** 585–601 (1980).